POLITECNICO DI TORINO
Repository ISTITUZIONALE

Validation of near infrared spectroscopy as an age-prediction method for plastics

(Article begins on next page)

07 August 2024

Corresponding Author: Professor Silvia Fiore, PhD

Corresponding Author's Institution: Politecnico di Torino

First Author: Ayah Alassali

Order of Authors: Ayah Alassali; Caterina Picuno; Tom Bebien; Silvia
Fiore, PhD; Kerstin Kuchta

Abstract: This work has two aims. Firstly, to validate the ability of
experimental models derived through near infrared spectroscopy for
acrylonitrile butadiene styrene (ABS), low-density polyethylene (LDPE),
polyethylene terephthalate (PET), and polypropylene (PP) in predicting
polymers' aging; focusing on the degree of oxidation. Secondly, to assess
the reliability of non-invasive age-predictive models on waste plastic
samples and on mechanically recycled samples. Aging time, temperature and
number of extrusion cycles were selected as independent variables to
build the aging-prediction models, where they were calibrated on samples
subjected to controlled conditions. The accuracy of the prediction models
was assessed on external samples (aged under known conditions) through
the cross correlation technique and the Root Mean Square Error (RMSE).
The models exhibited good collinearity for the aging temperature and the
number of extrusion cycles factors for all tested polymers, but not for
the aging time factor. The RSME value of the aging time factor was far
from zero for all polymers. Plastic waste samples provided analogous
results; the aging time estimation was mostly negative in value. The
estimations of aging time and number of extrusion cycles were always
positive in values, where the most reasonable aging factor estimation was
the number of extrusion cycles.

- We investigated NIR spectroscopy ability to predict the oxidation degree of polymers
- Aging-prediction models were experimentally derived for ABS, PE, PET and PP
- Aging time, temperature and no. of extrusion cycles were the independent variables
- The models were calibrated on artificially aged samples and waste polymers
- The no. of extrusion cycles proved to be a key parameter for the reliability of the models

1 **Validation of near infrared spectroscopy as an age-prediction method**

2 **for plastics**

3

4 Ayah Alassali [a], Caterina Picuno [a], Tom Bébien [b], Silvia Fiore [c, *], and Kerstin Kuchta [a]

5

6 [a] TUHH – Hamburg University of Technology, Institute of Environmental Technology and

7 Energy Economics, Waste Resources Management, Harburger Schlossstr. 36, 21079

8 Hamburg, Germany

9 [b] National Institute of Applied Sciences of Lyon (INSA), 20 Avenue Albert Einstein,

10 69100 Villeurbanne, France

11 [c] DIATI (Department of Engineering for Environment, Land and Infrastructures),

12 Politecnico di Torino, 24, corso Duca degli Abruzzi, 10129 Turin, Italy

13

14 ***Corresponding author:** prof Silvia Fiore, DIATI, Politecnico di Torino, Corso Duca

15 degli Abruzzi, 24; 10129, Torino, Italy; Email: silvia.fiore@polito.it; Phone: +39 011

16 0907613

17

Abstract

19 This work has two aims. Firstly, to validate the ability of experimental models derived

20 through near infrared spectroscopy for acrylonitrile butadiene styrene (ABS), low-density

21 polyethylene (LDPE), polyethylene terephthalate (PET), and polypropylene (PP) in

22 predicting polymers' aging; focusing on the degree of oxidation. Secondly, to assess the

23 reliability of non-invasive age-predictive models on waste plastic samples and on

24 mechanically recycled samples. Aging time, temperature and number of extrusion cycles

25 were selected as independent variables to build the aging-prediction models, where they

26 were calibrated on samples subjected to controlled conditions. The accuracy of the

27 prediction models was assessed on external samples (aged under known conditions)

28 through the cross correlation technique and the Root Mean Square Error (RMSE). The

29 models exhibited good collinearity for the aging temperature and the number of extrusion

30 cycles factors for all tested polymers, but not for the aging time factor. The RSME value

31 of the aging time factor was far from zero for all polymers. Plastic waste samples

32 provided analogous results; the aging time estimation was mostly negative in value. The

33 estimations of aging time and number of extrusion cycles were always positive in values,

34 where the most reasonable aging factor estimation was the number of extrusion cycles.

35
36
37 **Keywords:** FTNIR spectroscopy; polymer aging; polymer degradation; plastic waste;

38 prediction models

39 ## 1. Introduction

40 Plastics have become an environmental challenge, even though they do not generally

41 possess a direct hazard to the environment. Their environmental footprint results from

42 the consumption of non-renewable resources, in addition to being non-degradable

43 (Sánchez and Collinson 2011). The extensive application of plastics creates a challenge

44 connected to the waste management of the related flows. Moreover, the fact that a

45 considerable fraction of the produced plastic is intended for single-use disposable

46 applications (Hopewell et al. 2009) and mainly in form of films for household and

47 industrial applications (Horodytska et al. 2018) exacerbates an already critical

48 framework. Municipal solid waste management integrated systems are generally defined

49 through the hierarchy of prevention, reuse, recycling, and recovery and disposal, in

50 decreasing order of priority (Denise Reike et al. 2018). The adoption of the circular-

51 economy concept on waste plastics compels the application of recycling activities (M.K.

52 Eriksen et al. 2018).

53 There are essentially four types of plastic recycling, categorized as primary (re-

54 extrusion), secondary (mechanical), tertiary (chemical recycling) and quaternary (energy

55 recovery) (Yu et al. 2016; Al-Salem et al. 2009). Mechanical recycling of plastics is most

56 appropriate when polymers are separately collected from contaminated source (Ragaert

57 et al. 2017). Chemical recycling represents processes able to recover synthesis

58 monomers or feedstock chemicals by depolymerization. Whereas quaternary recycling

59 or energy recovery is particularly utilized if plastics cannot be mechanically recycled or

60 re-extruded due to contamination, separation difficulties, or significant degradation

61 (Ragaert et al. 2017). This study focused on the mechanical recycling of plastics, since

62 this process is by far the most commonly applied at industrial level for material recovery

63 (Al-Salem et al. 2009). Generally, material's quality should be maintained during

64 reprocessing and use as a subsequent product; therefore mechanical recycling is often

65 limited to selected types of plastic wastes such as Polyethylene terephthalate (PET)

66 bottles (Barlow and Morgan, 2013). The recycling of other types of polymers can be

67 more complex, due to the wide variety of grades, poor recovery, cross-contamination,

68 and downgrading in quality (Hopewell et al. 2009). The common difficulties related to

69 mechanical recycling are the heterogeneity of plastic wastes and the deterioration in

70 polymers' properties due to use and aging (Brandrup 1996; Perugini et al. 2005; Ragaert

71 et al. 2017). Polymer degradation can cause changes in chemical, physical and

72 mechanical features (Beninia et al. 2011; Anne Shayene Campos de Bomfim et al.

73 2019). Polymeric surface can also be attacked by material weathering (temperature,

74 humidity and light), microorganisms and chemical solutions (Alassali et al. 2018a;

75 Picuno et al. 2019a; Picuno et al. 2019b). Polymer degradation; occurring due to thermal

76 oxidation mechanisms is the focus of this study, as these mechanisms are typically

77 activated when the polymer is exposed to environmental conditions as well as to

78 elevated temperatures (i.e. during extrusion), in presence of oxygen (Izdebska 2016). As

79 a consequence, integrating systems that are able to determine the material quality and

80 degree of degradation in the industrial recycling scheme could strongly improve the

81 recycling process.

82 In a previous study, Near Infrared (NIR) spectroscopy was employed to propose

83 polymers' degradation-prediction models, those able to predict plastic aging by focusing

84 on the degree of oxidation (Alassali et al. 2018b). NIR spectroscopy was chosen due to

85 its wide application in plastic sorting facilities (Huth-Fehre et al. 1995; Wahab et al.

86 2006; Masoumi et al. 2012; S. Brunner et al. 2015) and due to its fast, accurate, and

87 non-destructive features (Blanco and Villarroya 2002). This work is a follow-up to the

88 previously conducted study by (Alassali et al. 2018b) and it aims at validating the

89 generated models and their ability in predicting polymers' degree of thermal oxidation. In

90 details, the prediction capability of the generated models was verified by the cross-

91 validation technique (Pasquini 2003), a basic statistical technique used for estimating

92 the predictive performance of a model (Bishop 2006) that typically relies on a small

93 dataset (Goodfellow et al. 2016). In order to achieve the validation of the aging-

94 prediction models—generated for the polymers polypropylene (PP), low-density

95 polyethylene (LDPE), polyethylene terephthalate (PET), and acrylonitrile butadiene

96 styrene (ABS), discretely—four sets of samples of virgin polymers were aged under

97 controlled conditions. The applied aging method simulates environmental conditions, yet

98 accelerated.   At molecular level, the thermo-oxidative degradation of the studied

polymers is a process accomplished with exposing the material to elevated temperatures in the presence of oxygen (Song et al. 2014). Consequently, a variation in the polymeric structure is provided as a result of compound's oxidation. The thermal oxidation rate and extent of each polymer are unique, which generally depend on the chemical structure and the stability of the polymeric chains (Alassali et al. 2018b). In this study, virgin material (free of additives and stabilizers) was used. This was important to decrease the number of variables in building the aging models. Certainly, different additives, stabilizers and coloring agents may contribute to the degree of degradation and hence to the generated mathematical models. However, this study focused on evaluating the possibility of producing aging-prediction models, and re-applying them on external samples (treated differently).

The second aim of this study was to utilize the validated age-prediction models to forecast the degree of thermal oxidation (aging) of plastic waste samples (deriving from e-waste) as well as on mechanically recycled samples, in order to test the viability of implementing the models on industrial-scale for the purpose of material recovery for recycling. To our knowledge this study is the first to investigate the reliability of non-invasive age-predictive models on waste plastics. Compared to the previous study (Alassali et al., 2018a), this work exhibits the following progresses: (I) a different and more complex validation approach was adopted, (II) a significant factor (number of extrusion cycles) was included to account for plastic aging by processing, and (III) the generated models were tested on real waste samples (derived from waste electrical and electronic equipment)

2.   Materials and Methods

123   **2.1. Materials**

124   *2.1.1.   Virgin plastic samples under controlled aging condition*

125   Virgin polymers (i.e. polymers free of additives) were either oven-aged under controlled

126   conditions—which means at defined temperature and duration (to simulate thermo-

127   oxidative effects)—or extruded (to simulate plastic mechanical processing) for the

128   purpose of validation. The same materials used in creating the aging models (Alassali et

129   al. 2018b) were also used for their cross-validation:

130   -   cylindrical granules of ABS from POLYLAC PA-747 - CHI MEI CORPORATION;

131   -   granules of PET, provided from NEOPET 82 FR - INEOS Olefins and Polymers

132   Europe;

133   -   cylindrical granules of LD-PE, provided from INEOS Olefins and Polymers

134   Europe; and

135   -   pellets of PP, provided from Olefins and Polymers Europe.

136

137   *2.1.2.   Plastic waste samples*

138   The second set of samples was obtained from an e-waste collection point in the city of

139   Hamburg (Germany). Ten items of different brands were selected, and only their plastic

140   components were considered in this study (see Table 1). The polymers of each

141   component were identified as specified in section 2.5.2.

142   Table 1. Description of the plastic waste samples deriving from e-waste units

Identified in the	e-waste unit	Image	Color	Polymer

study as				type
PP-1	Lamp cup		White	PP
PP-2	Water container of coffee maker		Transparent	PP
PP-3	Base of coffee maker		White	PP
PP-4	Closure of a juicer		White	PP
PP-5	Water container of an iron		White to transparent	PP
PP-6	Inner part of an iron		White	PP

ABS-1	Hand mixer		White	ABS
ABS-2	Case of digital clock radio		White-yellowish	ABS
ABS-3	Router case		White	ABS
ABS-4	Router case		White	ABS

143

2.2. Plastic aging-prediction models

145 As was explained in (Alassali et al. 2018b), aging-prediction models were created

146 utilizing the NIR spectra (obtained from a Bruker Optics FT-NIR spectrometer MPA,

147 Multi-Purpose Analyzer) of differently aged virgin polymers.

148 As a first step, controlled thermal aging of the material was conducted in a BINDER

149 oven, where two aging factors were considered (i.e., temperature and time), to simulate

150 the thermo-oxidative degradation of plastics during their use in accordance with ASTM-

151 F1980-07. The plastic aging-prediction models were generated depending on the

152 relation between the experimental aging parameters (i.e., time (h) and temperature (°C))

153 and the NIR spectra. The NIR spectra of differently aged polymers exhibited specific

154 variations in the absorbance intensity, related to changes taking place in the materials

155 chemical structure due to oxidation, in other words degradation. This can be assumed

156 with confidence, since the material used to build the models is virgin, without any

157 additives and stabilizers. The dependent variable was the absorbance at a number of

158 wavelengths, while the independent variables were the properties identified for the

159 study: time of exposure and temperature. PLS (Partial Least Squares) chemometric

160 algorithm could derive the empirical spectroscopic models for each polymeric material

161 (PET, ABS, LDPE and PP) after being aged at different conditions. This procedure

162 simultaneously reduced the amount of the spectral data and tried to find a regression

163 over the data. The underlying basis for the models and putative mechanisms of oxidation

164 was based on the observed spectral changes and by applying the principal component

165 analysis (PCA). After collecting the spectra, the modelling procedure was realized using

166 OPUS software. The "Quant 2 Method" option was used to apply a PLS regression on

167 the data points, where the aging parameters were inserted in relation to the NIR spectra

168 by the operator. Furthermore, the models were optimized through processing the data

169 points by the software OPUS to enhance the data fitting. The processing included data

170 pre-treatment. The different pre-treatment methods were semi-automatically selected,

171 where the PLS model (created by OPUS) provided suggestions (by proposing data

172 treatment methods and selecting regions of wavenumbers), after which, the operator

173 optimized the selection based on the obtained statistical evaluation. As a result, and due

174 to considering two aging factors, two linear models for every polymer were generated;

175 estimated aging time (h) and aging temperature (°C) of each sample could be obtained

176 by mathematical relations.

177 To get one linear relation between model-predicted parameters and experimental

178 parameters, thermo-oxidative aging time was calculated following Equation (1); once

179 applying the model-predicted aging parameters and a second time applying the

180 experimental aging parameters, finally they were plotted against each other. Thermo-

181 oxidative aging was calculated applying the concepts of chemical reaction kinetics

182 (Murray et al. 2013). It was assumed that the accelerated thermo-oxidative aging roughly

183 corresponds to doubling the aging rate for each increase of 10 °C (Shimada and Kabuki

184 1968; Boldizar and Möller 2003), hence, a Q10 value of 2 was used in Equation (1)

185 (Mandal et al. 2014; Alassali et al. 2018b; Alassali et al. 2018a). This relation is polymer

186 dependent; hence different models are expected to be obtained for different polymers.

187 $$t_{(accelerated)} = t_{real} \times Q10^{(T_{aging} - T_{ambient})/10} \qquad (1)$$

188 Where,

189 $t_{(accelerated)}$: accelerated aging time (in days),

190 $t_{(real)}$: the real aging time applied, using accelerated conditions (in days),

191 Q10: accelerated aging factor (here 2 is considered (Murray et al. 2013)),

192 $T_{(aging)}$: the aging temperature applied in the treatment process (°C),

193 $T_{(ambient)}$: the ambient temperature (°C).

194 The aging-prediction models explained in (Alassali et al. 2018b) (see Figure 1) were

195 used in this study with the aim of cross-validation (Equations 2-5), by predicting real (i.e.

196 experimental) aging parameters from the provided model-proposed aging parameters.

197
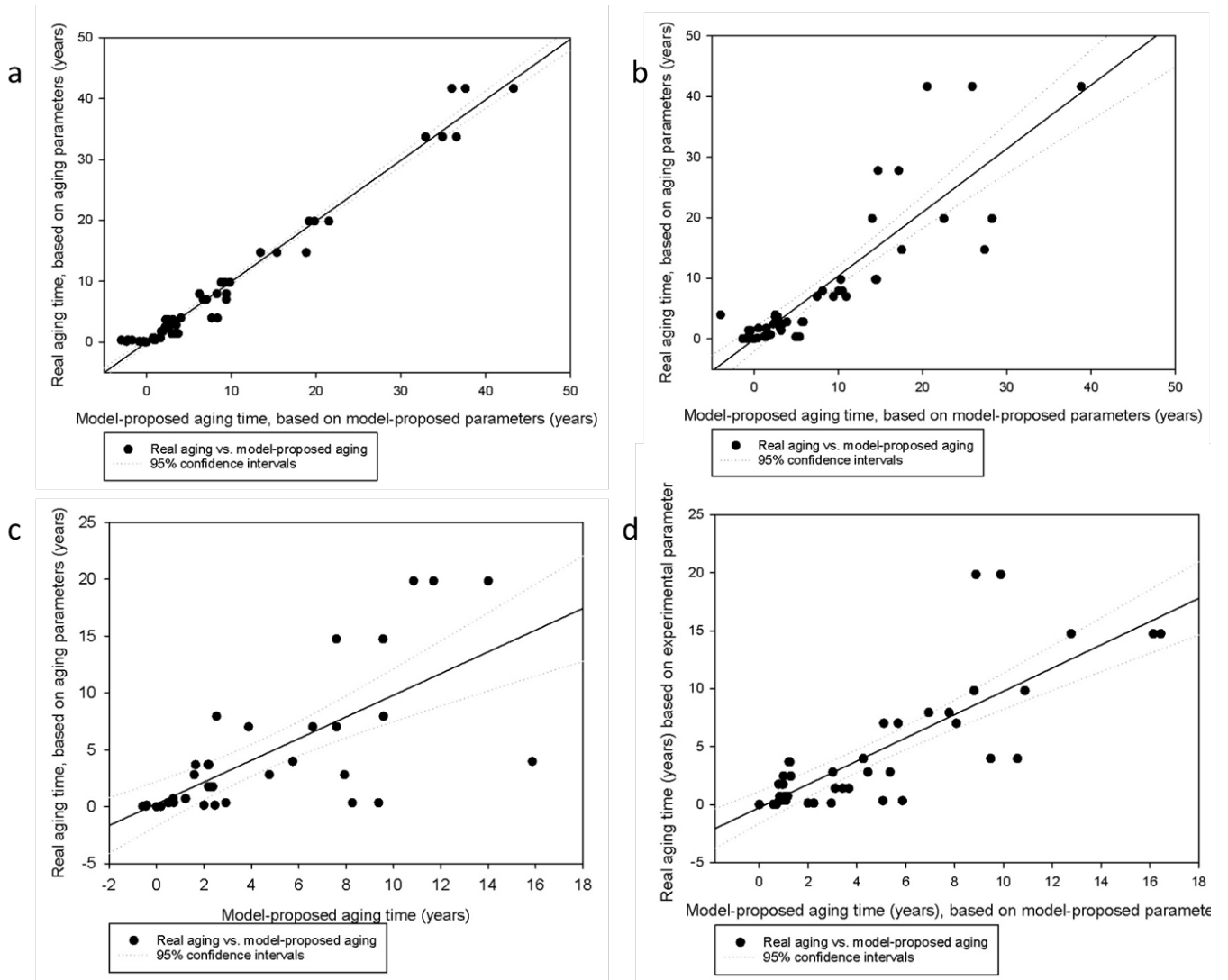
Figure 1. Calculated real aging time versus calculated model-proposed aging time: (a) ABS, (b) PET, (c) PP and (d) PE (Alassali et al. 2018b).

ABS: $Real\ ageing = 0.9961\ x\ Model\ predicted\ aging - 0.023$ (2)

PET: $Real\ ageing = 1.049\ x\ Model\ predicted\ aging - 0.0771$ (3)

PP: $Real\ ageing = 1.0832\ x\ Model\ predicted\ aging - 0.341$ (4)

PE: $Real\ ageing = 1.0016\ x\ Model\ predicted\ aging - 0.251$ (5)

206

11

207

2.3. Description of the models' validation technique

209 The objective of validating the generated NIR-based aging models, as any other

210 analytical procedure, is to demonstrate that it is suitable for its intended purpose (Broad

211 et al. 2002). Hence, the accuracy of the generated models needed to be evaluated (Pojić

212 et al. 2012), in this case by measuring how well the NIR prediction value match a given

213 reference value that is experimentally obtained. In many applications based on statistical

214 analysis, cross-validation is one of the simplest and most commonly reproduced

215 methods for estimating the prediction accuracy, therefore the error of a model (Hastie et

216 al. 2009). Given a specific and sufficiently large set of data, a fraction of the dataset

217 could theoretically be used for building the model, whereas the other part of the dataset

218 could be utilized as a validation test set. Moreover, there is another method for cross-

219 validation, which is called leave one out cross-validation (Öğütcü et al. 2012). However,

220 it is often the case in studies, like the present one, where the dataset is not big enough

221 to allow for its splitting. In order to overcome this issue and still be able to validate the

222 models in this study, the following 6-steps validation technique was applied to test the

223 models' accuracy:

224   1. The models to be validated were identified and equations describing each model

225   were derived (Equations 2-5);

226   2. New, independent sample sets of virgin and pure material were assimilated by the

227   application of thermal aging under defined conditions;

228   3. The newly created independent test sets were cross-validated with the before

229   generated PLS aging-prediction models;

230   4. The OPUS software was used to transform the NIR spectra into numerical values;

231   5. The model-proposed parameters were used to calculate the real aging

232   parameters following the linear mathematical relation created for age-prediction

233   (Equation 2-5);

234   6. The real aging parameters (as were calculated in step 5) were compared to

235   experimental aging parameters (applied in the lab) and the accuracy was

236   statistically tested.

237   The above-mentioned steps are described in detail in section 2.4.

238

239   **2.4. Model's accuracy statistical evaluation by cross-validation**

240   A test set of pure samples was acquired for each material by applying specific aging

241   temperature and aging time in a BINDER oven, as described in Table A in the

242   supplementary data. The test samples were analyzed through a Bruker Optics Fourier

243   Transform near infrared (FT-NIR) spectrometer MPA (Multi-Purpose Analyzer) and

244   acquired spectra were further processed and analyzed with OPUS spectroscopy

245   software from Bruker. The spectra of each test sample (described in Table A) were

246   cross validated with the corresponding aging models resulting in model-proposed aging

247   time (h) and model-proposed aging temperature (°C). Equation (1) was applied to

248   combine both parameters to calculate the model-proposed thermo-oxidative aging time

249   (expressed in years). The real thermo-oxidative aging time values for each polymer

250   were then calculated following the Equations 2, 3, 4 and 5 respectively, which results

251   were compared to the thermo-oxidative aging time calculated from the experimental

252   parameters (see the data repository, Table A) to calculate the models' aging-prediction

253   accuracy.

254   The accuracy of age prediction was assessed by calculating the mean error (ME) and

255   mean square error (MSE) (Prestwich et al. 2014; Azadi and Karimi-Jashni 2016), shown

256   in Equation (6) and Equation (7), respectively.

257 $$ME = \frac{1}{n} \sum_{i=1}^{n} (y_i' - y_i) \qquad (6)$$

258 $$MSE = \frac{1}{n} \sum_{i=1}^{n} (y_i' - y_i)^2 \qquad (7)$$

259   Furthermore, the Root Mean Square Error of Cross-Validation (RMSECV) (Equation (8)

260   (Chai and Draxler 2014)) was calculated for the test samples to characterize the model's

261   prediction accuracy.

262 $$RMSECV = \sqrt{\frac{\sum_{i=1}^{n} (y_i' - y_i)^2}{n}} \qquad (8)$$

263   where:

264   y_i = real thermo-oxidative aging time (using experimental values)

265   y_i' = real thermo-oxidative aging time estimated by the generated model

266   n = number of data points

267

268   **2.5. Creating a global polymer aging-prediction model**

269   *2.5.1. Including the extrusion effect in the polymer thermo-oxidative aging model*

270   Mechanical recycling of post-consumer plastics consists of sorting the material by

271   polymer type and color, shredding, washing, drying, possibly sorting once more the

272   resulting flakes and then extruding them in order to be transformed into granules. The

273   generated granules can be further molded to form specific consumer products. In the

274   context of this research, three extrusion cycles were performed. The first extrusion cycle

275   of virgin granules represented the first production process. The second extrusion cycle

276   was considered as a first recycling cycle, and the third extrusion resembled a second

277   cycle of recycling. Mechanical extrusion was performed using HAAKE^{TM} Rheomex CTW

278   100 OS Twin Screw Extruder.

279   First, the abovementioned models were applied to predict the age of extruded samples

280   to evaluate for the possibility of using the same models to predict the age (degree of

281   oxidation) of extruded polymers. As the models failed to efficiently and reproducibly

282   predict material aging after being extruded, new aging models were built, this time

283   including three parameters instead of two: heating temperature (°C), heating time (h)

284   and the number of extrusion cycles. These three parameters could not be combined in

285   one equation, therefore Equation (1) was not utilized and a model for each parameter

286   was independently built.

287

288   *2.5.2.   The application of the global aging-prediction models to forecast the*

289   *degree of waste material oxidation*

290   Plastic samples originated from e-waste were identified, sorted and separately shredded

291   by a Retsch Cutting Mill SM 300 to a size below 4.0 mm. The shredded samples were

292   analyzed by Bruker Optics FT-NIR spectrometer and acquired spectra were further

293   processed and analyzed with OPUS spectroscopy software. The spectra were cross

294   validated with the corresponding aging models, where a model-predicted aging time (h),

295   aging temperature (°C) and number of extrusion cycles for each test sample were

296   respectively provided.

3.   Results and Discussion

After aging, changes in the chemical structure were observed, identified by changes in the absorbance intensity of the NIR spectra of differently aged polymers. Multivariate calibration algorithms like PLS correlate spectral intensity (absorbance values) in specified wavelength regions with experimentally obtained aging parameters (time and temperature in this study). The calibration work, entirely achieved by Quant 2 Method. The results were obtained as data points; provided value of the parameter of interest versus the model-predicted value. The applied relation was PLS, hence, the data points generated a linear mathematical relation (shown in Figure 1 and Equations 2-5). For the cross-validation, the method developed to generate the models was retrieved and the spectral data of the test samples were automatically processed (every polymer was separately processed by its own mathematical relation). The software returned values of respective aging parameters, as the model estimates. The model-predicted values were plotted against the real values; this is presented in Figures 2 (a, c) and 3 (a, c), as black stars. The deviation between the plotted test values and model's relation (Figures 2 (a, c) and 3 (a, c), grey circles) could give a quantifiable evaluation of the prediction accuracy.

3.1. Aging time and temperature effects on the calculated thermo-oxidative aging

Thermo-oxidative degradation becomes increasingly important as the exposure temperature and time increase, delivering distinctive changes for each polymer.

Overall, the model-predicted thermo-oxidative aging time increased by increasing each

16

319   of the applied aging factors. For all models, the model-predicted aging temperature (°C)

320   was more accurately estimated than the model-predicted aging time (h). Moreover, at

321   higher aging temperatures, the thermo-oxidative aging rate increased more significantly

322   by increasing the experimental aging time. Simultaneously, the aging-prediction

323   accuracy decreased when elevated temperatures were applied, as was indicated by the

324   calculated RMSE values, especially for PET, PP and PE. The higher the RMSE value,

325   the lower the model's accuracy. For PET, RMSE increased from 0.98 for samples aged

326   at 85 °C to 9.01 for samples treated at 120 °C, for PP, RMSE increased from 0.85 for

327   samples aged at 85 °C to 6.51 for samples treated at 120 °C and PE it increased from

328   1.15 for samples treated at 85 °C to 6.21 for samples treated at 120 °C. This indicates

329   that the prediction accuracy decreases at higher aging temperatures, which could be

330   attributed to the non-linear effect of elevated temperatures on the degradation rate of the

331   tested polymers, where PLS method was assumed.

332   **3.2. Aging models' accuracy assessment by cross-validation**

333   *3.2.1.   ABS*

334   Figure 2.a shows an accurate estimation of the model-predicted thermo-oxidative aging

335   time of ABS (MSE = 0.90) at an experimental thermo-oxidative age lower than 5 years.

336   Yet, the overall age-prediction accuracy of the selected sample-set showed a slight

337   decrease (MSE = 2.42), which was due to the impreciseness in age estimation for the

338   sample treated at 120 °C for 336 h, possibly due to range of material coloration. Cross-

339   validation was performed by calculating the thermo-oxidative aging time twice:

340   (I)   Using the experimental aging parameters (i.e., time and temperature);

341   (II)   Using the model's estimated aging parameters to calculate relevant real aging

342   time (applying Equation (2); y = 0.9961 x + 0.023).

343 Values obtained from (I) and (II) were simultaneously plotted (see Figure 2.b). There is a

344 robust consistency in the values; they were generally overlapping. For the material aged

345 at 120 °C for 336 hours, the calculated model-based thermo-oxidative aging time was

346 higher by ~2 years for one sample and by ~4 years for another, indicating a range of

347 variation, yet less than what was observed by the rest of tested polymers. This variation

348 could be attributed to the possible non-linear oxidation behavior of the material, which

349 was interpreted by linear regression methods. The bias of the values was however

350 negligible (i.e., ME = 0.21). The overall RMSECV value (i.e., 1.51) shows a good age

351 estimation model.

352 *3.2.2. PET*

353 The cross-validation conducted on PET test samples indicated more compliance in the

354 aging region ≤11 years; model-predicted aging time varied for samples exposed to

355 thermo-oxidative aging parameters simulating aging time higher than 11 years (see

356 Figure 2.c). A high range of error between experimental thermo-oxidative aging time and

357 model-predicted thermo-oxidative aging time was obtained for the material aged at 120

358 °C for 408 h. The thermo-oxidative aging time calculated from the model's calibration

359 equation (y = 1.049 x − 0.0771 for PET) was plotted together with the real thermo-

360 oxidative aging time (calculated as per experimental parameters) to measure the degree

361 of agreement (see Figure 3.d). At aging temperature of 85 °C, the model showed high

362 prediction accuracy for all tested aging duration (bias values ranging between -0.94 and

363 1.01 only). For the thermo-oxidative aging at 120 °C, the aging time prediction accuracy

364 had an inverse relationship with the aging duration, where it was the lowest for the

material treated at 120 °C for 408 h. Generally, it was observed that the age prediction accuracy decreased with increasing the severity of aging (see Figure 2.d). When the samples treated at 120 °C for 408 h were excluded, the cross-validation of the PET aging model provided high accuracy, with ME value of 0.64 and MSE value of 4.48. Yet, the age-prediction accuracy of the PET aging model decreased significantly by cross-validating the mentioned sample; the MSE increased to 46.96, with an overall cross-validation RMSE value of 6.85. As well, this could be explained by the stability of PET under the applied aging conditions, which did not result in a linear aging behavior as estimated.
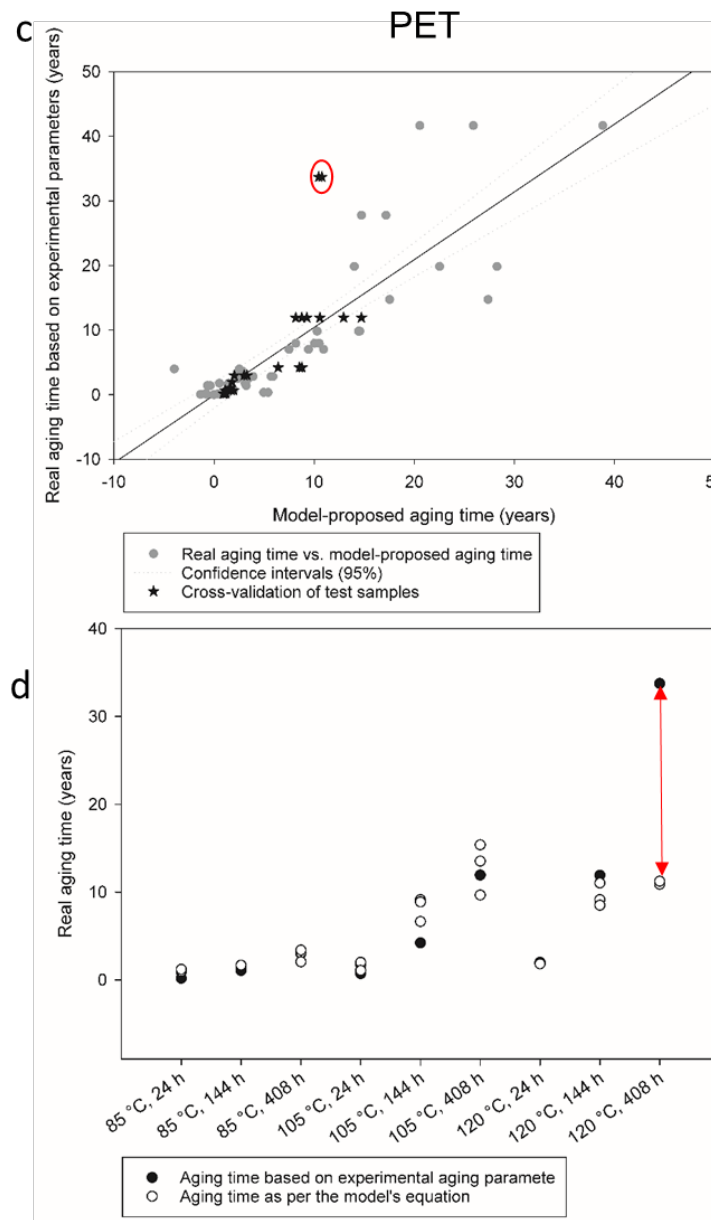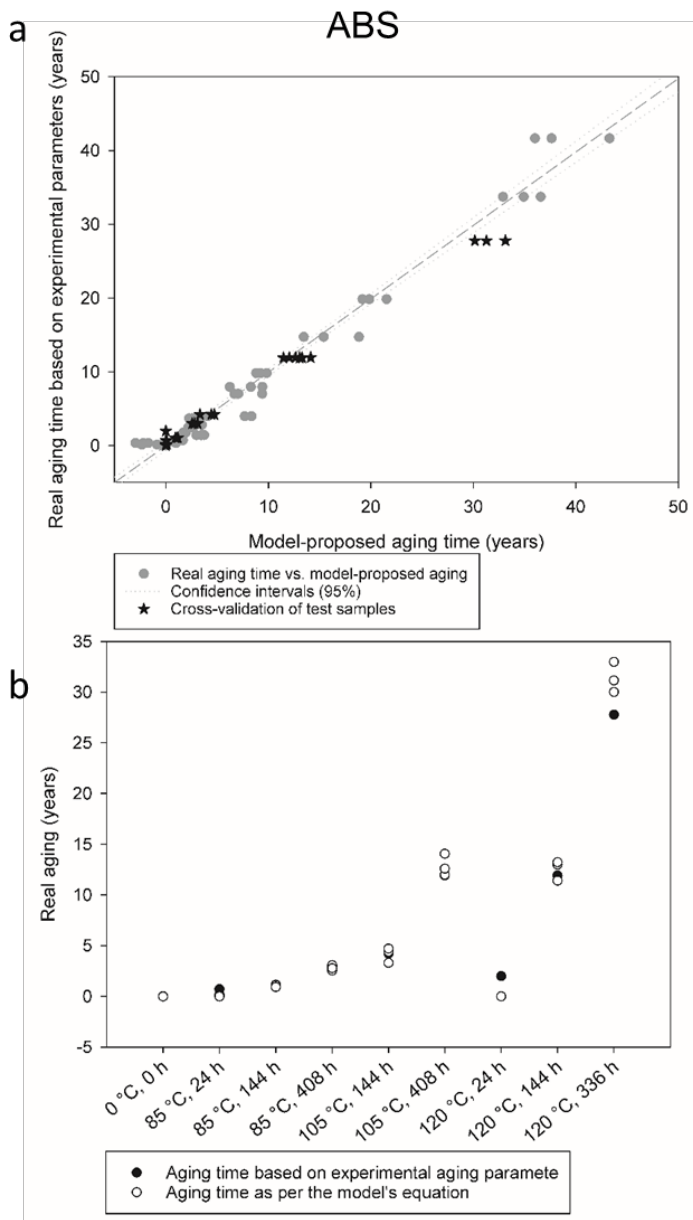
Figure 2. Left (a, b) for ABS and right (c, d) for PET: (a, c) Test samples cross-validated with the aging model, (b, d) comparison between real thermo-oxidative aging time obtained from experimental parameters and real thermo-oxidative aging time obtained from the generated regression model.

3.2.3.   PP

The PP aging model had a low collinearity, $R^2 = 0.64$ (see Figure 1 and Equation (4)),

381   yet this value was sufficient for a screening with wider error intervals (Krapf 2013). As

382   shown in Figure 3.a, higher aging-prediction accuracy of the test samples was obtained

383   for those that underwent short thermo-oxidative aging period (≤ 2 years). The real

384   thermo-oxidative aging of test samples was frequently accurately predicted applying the

385   model's formula (y = 1.083 x – 0.341), except for samples treated at 120 °C (see Figure

386   3.b). The MSE of the cross-validation for all samples treated at 85 °C and 105 °C was

387   2.0, which increased by about 6 folds when the samples treated at 120 °C were included

388   (i.e., MES value reached 11.83). This indicates that with increasing the severity of the

389   treatment, age-prediction accuracy decreases, while the effect of aging temperature was

390   more significant than the aging time. The overall cross-validation RMSE (3.44) value is

391   yet acceptable.

392

393   *3.2.4. PE*

394   As indicated in Figure 1 and Equation (5), the collinearity of the relation between

395   experimental thermo-oxidative aging time and model-predicted thermo-oxidative aging

396   was relatively low for PE (i.e., 0.66). However, the PE aging model in comparison to real

397   aging data showed good model estimation, with wider range of prediction error. As

398   shown in Figure 3.c, the cross-validation of test samples falls in the region of model's

399   confidence interval, except for the samples aged at 105 °C for 408 h and at 120 °C for

400   144 h, where the calculated thermo-oxidative aging for both conditions, applying

401   Equation (1), is 11.9 years. The model's anticipated aging was overestimated (by 2 to 5

402   years) for the samples aged at 105 °C for 408 h, where an age underestimation (by 6 to

403   8 years) was provided by the PE aging model for the samples aged at 120 °C for 144 h.

404   Following the regression model generated formula ($y = 1.016\,x - 0.251$), the calculated

405   real thermo-oxidative aging time showed negligible variations in comparison to the

406   experimental thermo-oxidative aging time for all test points, except for the above

407   mentioned two samples (see Figure 3.d). The overall cross-validation ME was

408   insignificant (i.e., 0.0182), yet the overall age-prediction accuracy was lower than what

409   was provided by the ABS aging model (MSE of 6.01). The calculated RMSE value for

410   the cross-validated samples indicated higher oxidation-prediction accuracy (i.e., 2.45) in

411   comparison to PET and PP aging models.

412
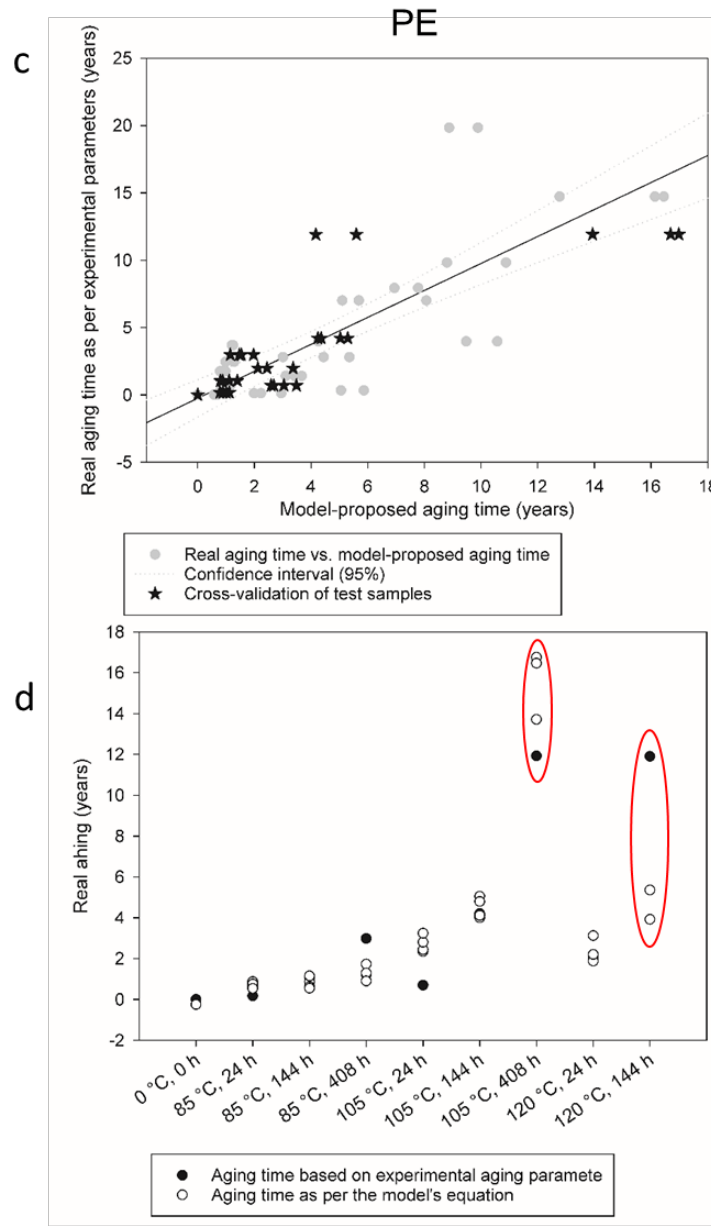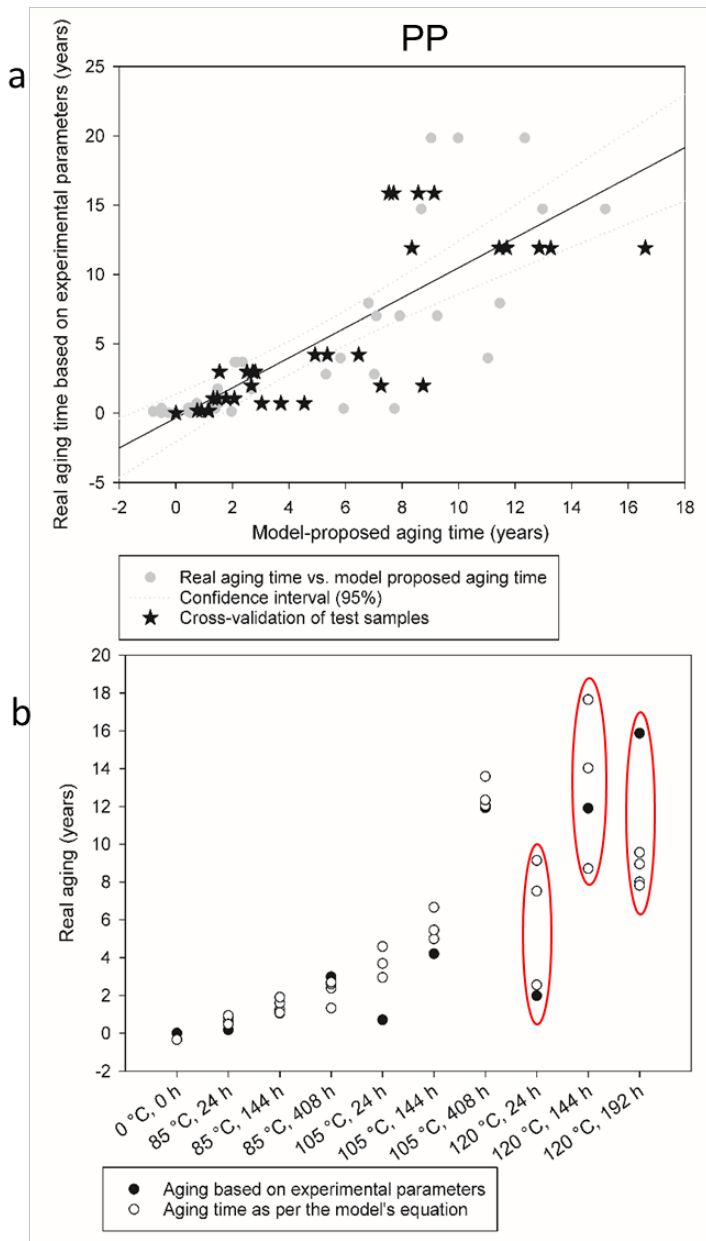
Figure 3. Left (a, b) for PP and right (c, d) for PE: (a, c) test samples cross-validated with the aging model, (b, d) comparison between real thermo-oxidative aging time obtained from experimental parameters and real thermo-oxidative aging time obtained from the generated regression model.

3.3. Comparison of the quality of the aging-prediction models

The aging-prediction models of different polymers (i.e., ABS, PET, PP and PE) were assessed by calculating the RMSECV of the test sets described in Table A in the supplementary material, which is calculated by weighing the deviation of the experimental thermo-oxidative aging values from the model's calculated thermo-oxidative aging time (using the created regression models in Figure 1). The RMSECV value calculated for the ABS aging model (1.51) was lower than the values calculated for PE and PP aging models (2.45 and 3.44, respectively), while the highest value was obtained for PET aging model (6.85). These results indicated that the performed cross-validation provided the best fitting for ABS aging model, however the model's quality decreased for other polymers aging models, to be the lowest for the PET aging model. Degradation process occurs due to the influence of thermal, chemical, mechanical, radiative and biochemical factors; resulting in deterioration of mechanical and physical properties of polymers. The degradation occurs due to changes in the main backbone or side groups of the polymer (Venkatachalam et al. 2012). The degradation of PE and PP could result in chain breakage and formation of radicals, which are easily oxidized. Therefore, it is expected to obtain an increase in C=C, C=O or C—OH bonds in the generated NIR spectra after material aging, in addition to the increase in the concentration of methyl groups (Alassali et al. 2018b). However, the models indicated that the oxidation rate of PE and PP is slower that what the model would predict, which resulted in low collinearity and reduced age estimation accuracy. In PET, the aromatic ring connected to a short aliphatic chain provides stiffness to the molecule. The lack of segmental mobility in the polymer chains results in relatively high thermal stability

443   (Venkatachalam et al. 2012). Nevertheless, the thermal degradation of PET was

444   reported to take place leading to cyclic oligomers and chain scission, resulting in vinyl

445   ester and acid end-groups (Holland and Hay 2002). As per the generated aging

446   prediction model for PET, the model aging time and aging temperature estimation had a

447   range of values, providing that the chemical stability of the polymer resulted in

448   inhomogeneous degradation performance. On the other hand, degradation of the

449   elastomeric polybutadiene phase (i.e., containing C=C) in ABS is initiated by hydrogen

450   abstraction from the carbon α to unsaturated bonds, resulting in hydroperoxide radicals

451   and producing carbonyl and hydroxyl products. Furthermore, degradation of the

452   styrene–acrylonitrile phase in ABS takes also place by thermo-oxidative degradation, yet

453   in lower rate (Tiganis et al. 2002a). Generally, the age-prediction model of ABS showed

454   a high accuracy and optimized linearity, which is attributed to the linear relation between

455   the degree of degradation of the polymer and the aging severity, which fits with the

456   linear regression methods being applied.

457   Comparing the RMSECV values of the test samples to what was obtained by the original

458   aging model described by (Alassali et al. 2018b), lower values were obtained for ABS,

459   PE and PP, whereas it was higher for PET. This could be attributed to the limited

460   number of test samples used in the cross-validation in comparison to the data points

461   used in constructing the models; having few samples, which were unable to capture the

462   model's trend, allowed for an elevated RMSECV value. Despite the bias in the predicted

463   thermo-oxidative aging time, the four models were able to provide an age estimation

464   tool.

465   **3.4. The application of the original age-prediction models as a tool of age**

466   **estimation of polymer samples**

467   *3.4.1.   Extruded samples*

468   The utilization of the age-prediction models was incompatible to predict degradation

469   (i.e., aging) of extruded samples. As shown in the data repository, Table B, the predicted

470   aging parameters were below zero, especially for ABS and PET. This was attributed to

471   the great change in color of these two polymers after extrusion (see Figure 4).

New granules   Extruded granules

ABS

PET

PP

PE

472
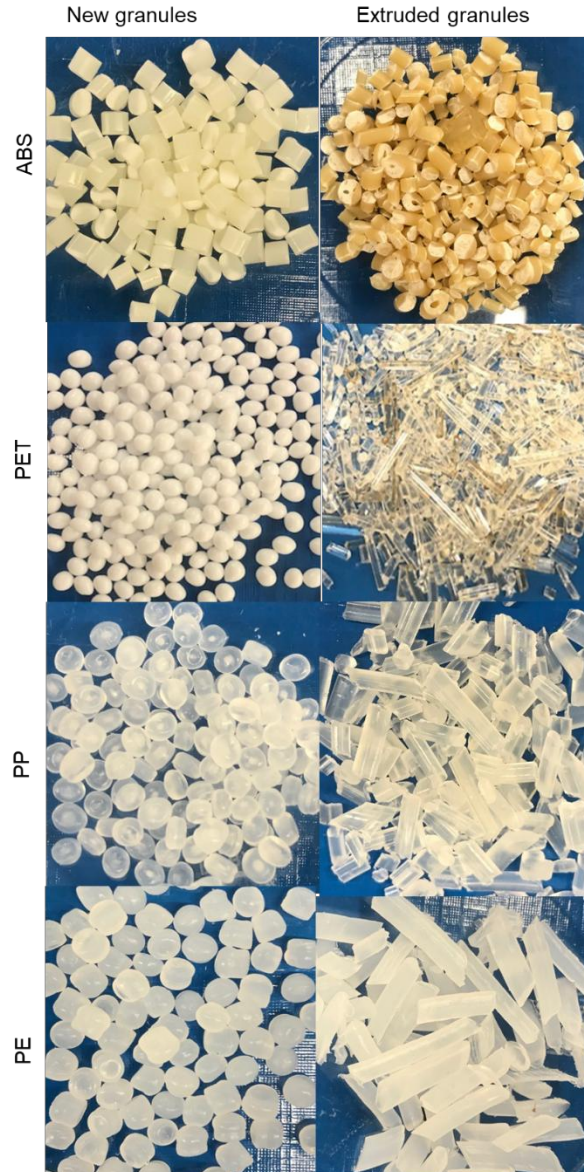
Figure 4. The change of color of polymers after extrusion

3.4.2.   Waste samples

As the data in the data repository, Table B showed, the model predicted negative aging temperatures for samples PP-2 and PP-5 (from Table 1), which resulted in a negative thermo-oxidative aging time (years) estimation. The predicted aging temperature of PP-1, PP-3, PP-4 and PP-6 was too high (above 1000 °C), which resulted in an aging time overestimation, especially for PP-6. This could be attributed to the effect of extrusion

480   and molding taking place during production, which has accelerated the thermo-oxidation

481   of the polymers and consequently resulted in intense coloration. For ABS, the aging

482   temperature of the material was mostly estimated to be negative, resulting in negative

483   values of thermo-oxidative aging time (years). The results support what was obtained in

484   extruded samples, where the granules color changes significantly by extrusion and

485   possibly molding. Not to forget the possible impact of stabilizers and antioxidants in the

486   plastics formulations to provide protection during processing or fabrication into finished

487   product (Dopico-García et al. 2011).

488   **3.5. Building a global polymer aging model**

489   In previous models, the effects of aging time and temperature were accounted.

490   However, in the production phase, polymers undergo harsher processing conditions,

491   where melting takes place during both, extrusion and molding. For this reason, the initial

492   models (including time and temperature factors) did not have the capacity to properly

493   predict thermo-oxidative behavior of consumer products (plastics derived from electrical

494   waste). Hence, the factor of number of extrusion cycles was additionally evaluated. For

495   this study, the number of extrusion cycles was restricted to 3. As can be seen in Figure

496   5, for each material (i.e., (a) ABS, (b) PET, (c) PP and (d) PE), three equations were

497   extracted, one to predict the aging time (h), a second one to predict the aging

498   temperature (°C) and a third one to predict the number of extrusion cycles (from left to

499   right in Figure 5).

500
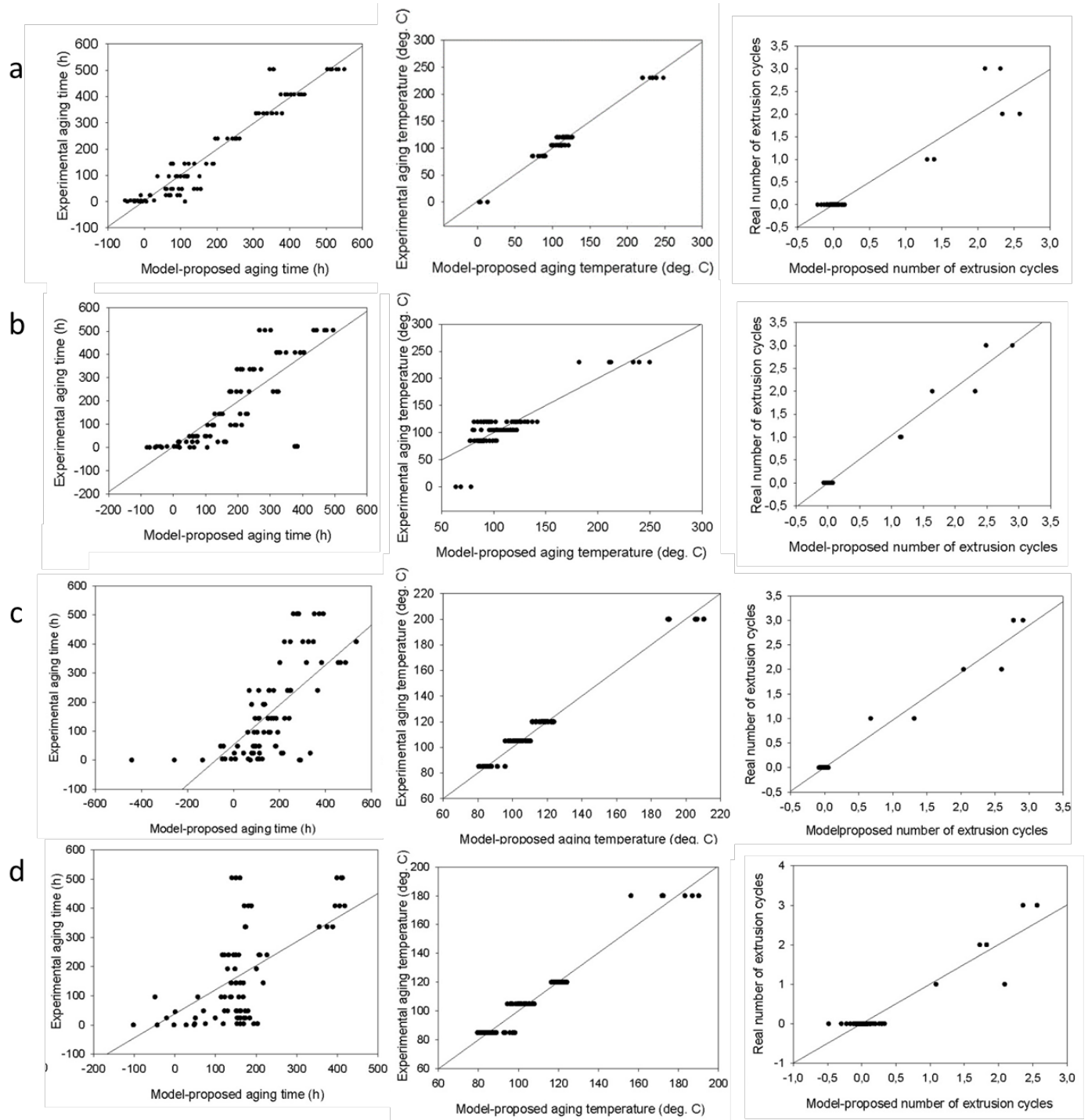
Figure 5. The global aging models created to predict materials' aging time (h), aging temperature (°C) and number of extrusion cycles (from left to right) for (a) ABS, (b) PET, (c) PP and (d) PE.

504 The generated models were evaluated by calculating the RMSE for each aging

505 parameter, which was calculated by accounting for the difference between the model-

506 proposed value and the experimental value for virgin test samples. The model

507 constructed for ABS was the most efficient in comparison to PET, PP and PE (see

508 Figure 6). The model was less accurate in estimating the aging time (h) in comparison to

509 all other parameters (components), for all tested materials (ABS, PET, PP and PE). The

510 RMSE value was, however, the lowest for ABS (47.48) and the highest for PP (125.56)

511 (Figure 6.a). Aging temperature prediction was significantly more precise for ABS, PP

512 and PE, where the RMSE of the PET model showed a significant increase (lowering the

513 model's estimation accuracy) (Figure 6.b). For all tested polymers, the estimation of the

514 number of extrusion cycles was considerably accurate (see Figure 6.c). This could be

515 attributed to the limited number of extrusion cycles applied (ranging from 0 to 3).

516 Moreover, the R^2 value was calculated for all parameters of the global aging models

517 (see Figure 6.d). For ABS the relation between experimental aging parameters and

518 model-proposed aging parameters was mostly collinear (i.e., 0.92 for aging time

519 component, 0.98 for aging temperature component and 0.91 for number of extrusion

520 cycles component). The collinearity of the relation between real aging time and model-

521 proposed aging time for PET was relatively low (0.66), yet allowing for the application of

522 approximate calibration (Krapf 2013). The R^2 value increased significantly for the

523 extrusion cycle component for the PET global aging model to reach 0.98. For PP and

524 PE, the global aging model indicated poor aging time estimation, the R^2 values for the

525 aging time component for PP and PE were 0.46 and 0.40, respectively. Yet, for the

526 aging temperature component and number of extrusion cycles components, the R^2

527 values were both 0.98 for PP, indicating the model's applicability. The R^2 values were

30

528 similarly high for PE (i.e., for aging temperature component: 0.95 and for number of

529 extrusion cycles component: 0.90), allowing for the application of the model for different

530 purposes, covering quality insurance applications.
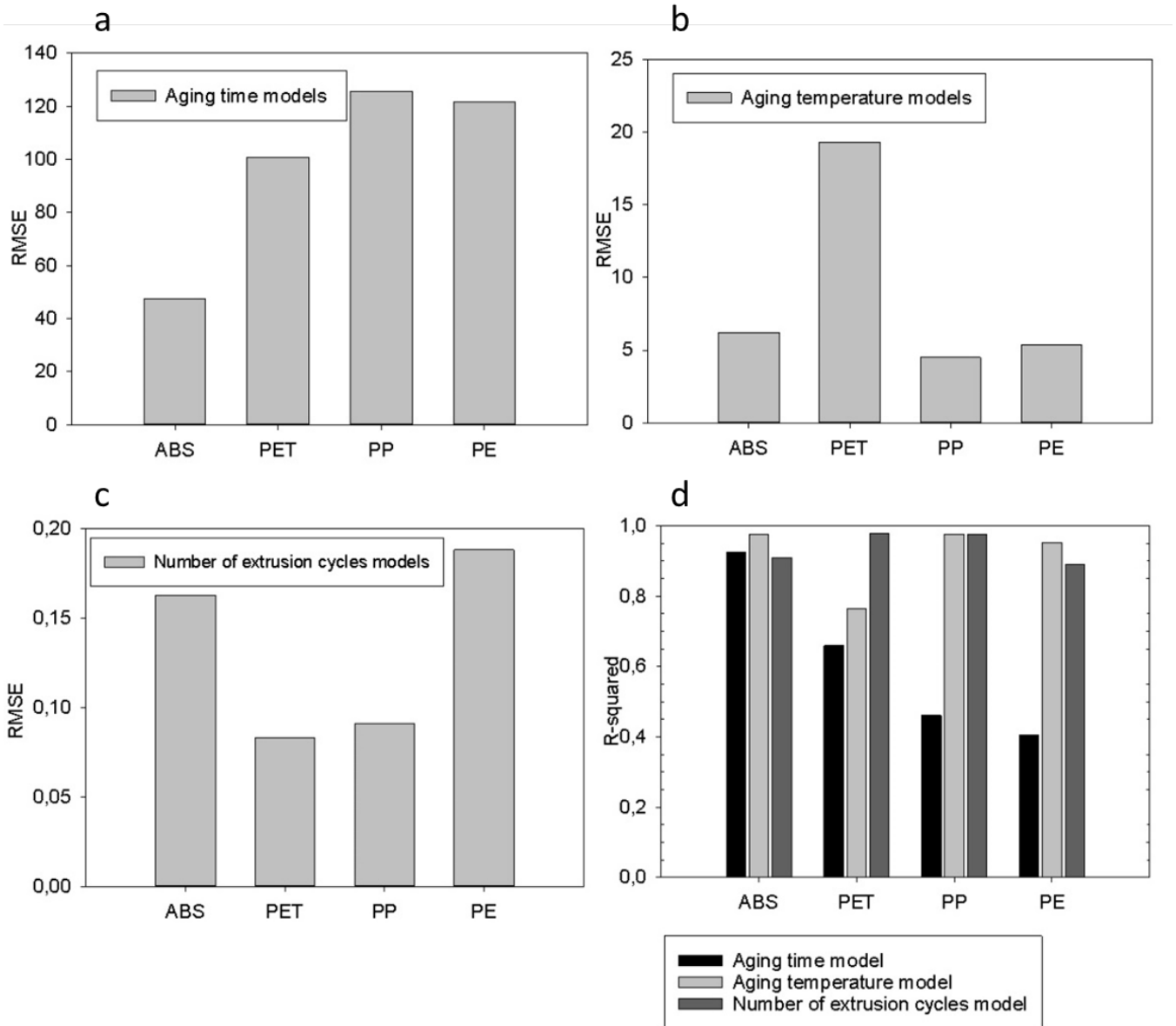
531

532 Figure 6. Evaluation of the global aging models for ABS, PET, PP and PE; (a) RMSE for

533 the aging time component, (b) RMSE for the aging temperature component, (c) RMSE

534 for the number of extrusion cycles component and (d) R^2-value for the three mentioned

535 components of the aging models.

536 *3.5.1.   The application of the global models to estimate the age of waste samples*

537 The aim of creating global aging models is to develop a quality control tool to assess the

538 quality of the recycling input material and, therefore, to improve the quality of recycled

539 material. The model-proposed aging time, aging temperature and number of extrusion

540 cycles were used to calculate the real aging time, aging temperature and number of

541 extrusion cycles following the equations provided by the generated global models. It can

542 be clearly seen from Table C (in supplementary material) that the models failed to

543 estimate the aging duration of the material, where values were either below zero

544 (especially for ABS polymer) or too high (PP-4 and PP-6). The predicted aging

545 temperature for ABS was 3 to 5 folds higher than that for PP, which is ascribed to the

546 material coloration. The estimation of the number of extrusion cycles for both materials

547 was reasonably acceptable; positive values in acceptable ranges were obtained.

548 **3.6.   Economic and environmental considerations**

549 This research has significant practical, economic and environmental consequences. Life

550 Cycle Analysis assessed the environmental benefits of plastic recycling, compared to

551 disposal in waste-to-energy facilities, and results were controversial (Huysveld et al.

552 2019; Faraca et al. 2019; Khoo 2019). Considering the economic outcomes, plastic

553 recycling could easily become economically too expensive (if the recycled product

554 exhibits low features and consequently low market value) to achieve a net benefit

555 compared to disposal. However, as a general statement, policy interventions supporting

556 plastics recycling, as well as technological changes and a transparent communication

557 and collaboration between all stakeholders are needed to enhance the recycling process

558 (Hahladakis and Iacovidou 2019). Nowadays, recycling is usually associated with higher

559 economic efforts than incineration due to higher labor needs and enhanced transport

560 and sorting costs, hence, proposing an available technique (NIR sorting) in order to

561 enhance the quality of plastic recycling should be of a great significance in industrial

562 applications.

563 ## 4. Conclusions

564 The aim of this study was to validate plastic aging-prediction models for their industrial

565 applicability, especially for material quality identification for recycling. A recent study

566 (Faraca et al. 2019) proved that if high quality of the recycled plastic is achieved, both

567 environmental savings and financial revenues are possible. Therefore the here

568 presented aging-prediction models could be of great help for material quality

569 identification in plastic sorting facilities.

570 The generated models showed effectiveness in age-estimation of experimentally aged

571 polymers. The ABS aging-prediction model was the most accurate among all tested

572 polymers, which was attributed to the quantifiable changes in the chemical structure

573 through aging. For other polymers (i.e., PET, PP and PE), although the accuracy of age-

574 estimation was lower, the models could still be applicable to estimate the age of

575 material, which was aged under controlled conditions. The original aging-prediction

576 models provided negative aging values for extruded ABS and PET samples.

577 Consequently, negative thermo-oxidative aging duration were calculated. Hence, new

578 aging-prediction models (i.e. identified as global aging-prediction models) were created,

579 including the factor of 'number of extrusion cycles'. Generally, these models exhibited a

580 good collinearity for the 'aging temperature' factor and the 'number of extrusion cycles'

581 factor. However, the 'aging time' factor of PET, PP and PE provided a collinearity lower

582 than 0.70. The models' estimation accuracy was also evaluated by calculating the

583 RMSE for each of the mentioned factors. The aging time factor was far from zero for all

584 tested polymers, yet the lowest value was obtained for ABS (47.48) and the highest for

585 PP (125.56). This was replicated when plastic waste samples were tested; the aging

586 time estimation was mostly negative in value, especially for ABS material. The

587 estimations of 'aging temperature and the 'number of extrusion cycles' were always

588 positive in values, where the most reasonable aging factor estimation was the 'number

589 of extrusion cycles'. All in all, the generated models need to be extended to include a

590 wider range of data, where further aging parameters, e.g. UV radiation (Picuno et al.

591 2019a) should be considered for the aim of including all possible forms and degrees of

592 degradation.

Acknowledgements

References

Alassali, A.; Moon, H.; Picuno, C.; Meyer, R. S.A.; Kuchta, K. (2018a): Assessment of polyethylene degradation after aging through anaerobic digestion and composting. In *Polymer Degradation and Stability* 158, pp. 14–25.

Alassali, Ayah; Fiore, Silvia; Kuchta, Kerstin (2018b): Assessment of plastic waste materials degradation through near infrared spectroscopy. In *Waste management* 82, pp. 71–81. DOI: 10.1016/j.wasman.2018.10.010.

Al-Salem, S. M.; Lettieri, P.; Baeyens, J. (2009): Recycling and recovery routes of plastic solid waste (PSW). A review. In *Waste management* 29 (10), pp. 2625–2643.

Anne Shayene Campos de Bomfim; Maísa Milanez Ávila Dias Maciel; Herman Jacobus Cornelis Voorwald; Kelly Cristina Coelho de Carvalho Benini; Daniel Magalhães de Oliveira; Maria Odila Hilário Cioffi (2019): Effect of different degradation types on properties of plastic waste obtained from espresso coffee capsules. In *Waste management* 83, pp. 123–130. DOI: 10.1016/j.wasman.2018.11.006.

Azadi, Sama; Karimi-Jashni, Ayoub (2016): Verifying the performance of artificial neural network and multiple linear regression in predicting the mean seasonal municipal solid waste generation rate: A case study of Fars province, Iran. In *Waste management* 48, pp. 14–23.

Beninia, KCCC; Voorwald, Herman Jacobus Cornelis; Cioffi, M. O.H. (2011): Mechanical properties of HIPS/sugarcane bagasse fiber composites after accelerated weathering. In *Procedia Engineering* 10, pp. 3246–3251.

Bishop, Christopher M. (2006): Pattern recognition and machine learning: springer.

35

622   Blanco, M.; Villarroya, INIR (2002): NIR spectroscopy: a rapid-response analytical tool.

623   In *TrAC Trends in Analytical Chemistry* 21 (4), pp. 240–250.

624   Boldizar, Antal; Möller, Kenneth (2003): Degradation of ABS during repeated processing

625   and accelerated ageing. In *Polymer Degradation and Stability* 81 (2), pp. 359–366.

626   Brandrup, J. (1996): Recycling and recovery of plastics. Munich, New York: Hanser.

627   Broad, Neville; Graham, Paul; Hailey, Perry; Hardy, Allison; Holland, Steve; Hughes,

628   Stephen et al. (2002): Guidelines for the development and validation of near-infrared

629   spectroscopic methods in the pharmaceutical industry. In *Handbook of vibrational*

630   *spectroscopy* 5, pp. 3590–3610.

631   Chai, Tianfeng; Draxler, Roland R. (2014): Root mean square error (RMSE) or mean

632   absolute error (MAE)?–Arguments against avoiding RMSE in the literature. In

633   *Geoscientific model development* 7 (3), pp. 1247–1250.

634   da Costa, Helson M.; Ramos, Valéria D.; Oliveira, Márcia G. de (2007): Degradation of

635   polypropylene (PP) during multiple extrusions: Thermal analysis, mechanical

636   properties and analysis of variance. In *Polymer Testing* 26 (5), pp. 676–684. DOI:

637   10.1016/j.polymertesting.2007.04.003.

638   Denise Reike; Walter J.V. Vermeulen; Sjors Witjes (2018): The circular economy: New

639   or Refurbished as CE 3.0? — Exploring Controversies in the Conceptualization of the

640   Circular Economy through a Focus on History and Resource Value Retention

641   Options. In *Resources, Conservation and Recycling* 135, pp. 246–264. DOI:

642   10.1016/j.resconrec.2017.08.027.

643   Dopico-García, M. S.; Castro-López, M. M.; López-Vilariño, J. M.; González-Rodríguez,

644   M. V.; Valentao, P.; Andrade, P. B. et al. (2011): Natural extracts as potential source

645   of antioxidants to stabilize polyolefins. In *Journal of Applied Polymer Science* 119 (6),

646   pp. 3553–3559.

647 Faraca, Giorgia; Martinez-Sanchez, Veronica; Astrup, Thomas F. (2019): Environmental

648   life cycle cost assessment: Recycling of hard plastic waste collected at Danish

649   recycling centres. In *Resources, Conservation and Recycling* 143, pp. 299–309.

650 Goodfellow, Ian; Bengio, Yoshua; Courville, Aaron (2016): Deep learning: MIT press.

651 Hahladakis, John N.; Iacovidou, Eleni (2019): An overview of the challenges and trade-

652   offs in closing the loop of post-consumer plastic waste (PCPW): Focus on recycling.

653   In *Journal of Hazardous Materials* 380, p. 120887.

654 Hastie, Trevor; Tibshirani, Robert; Friedman, Jerome (2009): The elements of statistical

655   learning: data mining, inference, and prediction, Springer Series in Statistics:

656   Springer New York.

657 Holland, B. J.; Hay, J. N. (2002): The thermal degradation of PET and analogous

658   polyesters measured by thermal analysis–Fourier transform infrared spectroscopy. In

659   *Polymer* 43 (6), pp. 1835–1847.

660 Hopewell, Jefferson; Dvorak, Robert; Kosior, Edward (2009): Plastics recycling:

661   challenges and opportunities. In *Philosophical Transactions of the Royal Society of*

662   *London B: Biological Sciences* 364 (1526), pp. 2115–2126.

663 Horodytska, O.; Valdés, F. J.; Fullana, A. (2018): Plastic flexible films waste

664   management – A state of art review. In *Waste management*. DOI:

665   10.1016/j.wasman.2018.04.023.

666 Huth-Fehre, Th; Feldhoff, R.; Kantimm, Th; Quick, L.; Winter, F.; Cammann, K. et al.

667   (1995): NIR-Remote sensing and artificial neural networks for rapid identification of

668   post consumer plastics. In *Journal of Molecular Structure* 348, pp. 143–146.

669 Huysveld, Sophie; Hubo, Sara; Ragaert, Kim; Dewulf, Jo (2019): Advancing circular

670   economy benefit indicators and application on open-loop recycling of mixed and

671   contaminated plastic waste fractions. In *Journal of cleaner production* 211, pp. 1–13.

672 Izdebska, Joanna (2016): Aging and Degradation of Printed Materials. In Joanna

673   Izdebska, Sabu Thomas (Eds.): Printing on Polymers: William Andrew Publishing,

674   pp. 353–370. Available online at

675   http://www.sciencedirect.com/science/article/pii/B9780323374682000221.

676 Khoo, Hsien H. (2019): LCA of plastic waste recovery into recycled materials, energy

677   and fuels in Singapore. In *Resources, Conservation and Recycling* 145, pp. 67–77.

678 Krapf, Lutz Christian (2013): Evaluation of near infrared spectroscopy to estimate

679   process parameters in anaerobic digestion of agricultural feedstocks. Technische

680   Universität München.

681 M.K. Eriksen; K. Pivnenko; M.E. Olsson; T.F. Astrup (2018): Contamination in plastic

682   recycling: Influence of metals on the quality of reprocessed plastic. In *Waste*

683   *management* 79, pp. 595–606. DOI: 10.1016/j.wasman.2018.08.007.

684 Mandal, Himadri S.; Knaack, Gretchen L.; Charkhkar, Hamid; McHail, Daniel G.; Kastee,

685   Jemika S.; Dumas, Theodore C. et al. (2014): Improving the performance of poly (3,

686   4-ethylenedioxythiophene) for brain–machine interface applications. In *Acta*

687   *biomaterialia* 10 (6), pp. 2446–2454.

688 Masoumi, Hamed; Safavi, Seyed Mohsen; Khani, Zahra (2012): Identification and

689   classification of plastic resins using near infrared reflectance. In *International Journal*

690   *of Mechanical and Industrial Engineering* 6, pp. 213–220.

691 Murray, Kieran A.; Kennedy, James E.; McEvoy, Brian; Vrain, Olivier; Ryan, Damien;

692   Cowman, Richard; Higginbotham, Clement L. (2013): The effects of high energy

693   electron beam irradiation in air on accelerated aging and on the structure property

694 relationships of low density polyethylene. In *Nuclear Instruments and Methods in*

695 *Physics Research Section B: Beam Interactions with Materials and Atoms* 297,

696 pp. 64–74.

697 Öğütcü, Mustafa; Aydeniz, Buket; Büyükcan, Mehmet Burak; Yılmaz, Emin (2012):

698 Determining frying oil degradation by near infrared spectroscopy using chemometric

699 techniques. In *Journal of the American Oil Chemists' Society* 89 (10), pp. 1823–1830.

700 Pasquini, Celio (2003): Near infrared spectroscopy: fundamentals, practical aspects and

701 analytical applications. In *Journal of the Brazilian chemical society* 14 (2), pp. 198–

702 219.

703 Perugini, Floriana; Mastellone, Maria Laura; Arena, Umberto (2005): A life cycle

704 assessment of mechanical and feedstock recycling options for management of

705 plastic packaging wastes. In *Environ. Prog.* 24 (2), pp. 137–154. DOI:

706 10.1002/ep.10078.

707 Picuno, Caterina; Alassali, Ayah; Sundermann, Michel; Godosi, Zoe; Picuno, Pietro;

708 Kuchta, Kerstin (2019a): Decontamination and recycling of agrochemical plastic

709 packaging waste. In *Journal of Hazardous Materials*, p. 120965.

710 Picuno, Caterina; Godosi, Zoe; Kuchta, Kerstin; Picuno, Pietro (2019b): Agrochemical

711 plastic packaging waste decontamination for recycling: Pilot tests in Italy. In *Journal*

712 *of Agricultural Engineering* 50 (2), pp. 99–104.

713 Pojić, Milica; Mastilović, Jasna; Majcen, Nineta (2012): The application of near infrared

714 spectroscopy in wheat quality control. In : Infrared spectroscopy-Life and biomedical

715 sciences: IntechOpen.

716 Prestwich, Steven; Rossi, Roberto; Armagan Tarim, S.; Hnich, Brahim (2014): Mean-

717 based error measures for intermittent demand forecasting. In *International Journal of*

718   *Production Research* 52 (22), pp. 6782–6791.

719   Ragaert, Kim; Delva, Laurens; van Geem, Kevin (2017): Mechanical and chemical

720   recycling of solid plastic waste. In *Waste management* 69, pp. 24–58.

721   S. Brunner; P. Fomin; Ch. Kargel (2015): Automated sorting of polymer flakes:

722   Fluorescence labeling and development of a measurement system prototype. In

723   *Waste management* 38, pp. 49–60. DOI: 10.1016/j.wasman.2014.12.006.

724   Sánchez, Arnau Carné; Collinson, Simon R. (2011): The selective recycling of mixed

725   plastic waste of polylactic acid and polyethylene terephthalate by control of process

726   conditions. In *European Polymer Journal* 47 (10), pp. 1970–1976.

727   Shimada, Junichi; Kabuki, Kimiaki (1968): The mechanism of oxidative degradation of

728   ABS resin. Part I. The mechanism of thermooxidative degradation. In *Journal of*

729   *Applied Polymer Science* 12 (4), pp. 655–669.

730   Song, Qilei; Cao, Shuai; Pritchard, Robyn H.; Ghalei, Behnam; Al-Muhtaseb, Shaheen

731   A.; Terentjev, Eugene M. et al. (2014): Controlled thermal oxidative crosslinking of

732   polymers of intrinsic microporosity towards tunable molecular sieve membranes. In

733   *Nature communications* 5, p. 4813.

734   Thomas S. Gates (Ed.) (1999): On the use of accelerated aging methods for screening

735   high temperature polymeric composite materials. 40TH Structures, Structural

736   Dynamics, and Materials Conference and Exhibit.

737   Tiganis, B. E.; Burn, L. S.; Davis, Paul; Hill, A. J. (2002a): Thermal degradation of

738   acrylonitrile–butadiene–styrene (ABS) blends. In *Polymer Degradation and Stability*

739   76 (3), pp. 425–434.

740   Tiganis, B.E; Burn, L.S; Davis, P.; Hill, A.J (2002b): Thermal degradation of acrylonitrile–

741   butadiene–styrene (ABS) blends. In *Polymer Degradation and Stability* 76 (3),

742   pp. 425–434. DOI: 10.1016/S0141-3910(02)00045-9.

743   Venkatachalam, S.; Nayak, Shilpa G.; Labde, Jayprakash V.; Gharal, Prashant R.; Rao,

744   Krishna; Kelkar, Anil K. (2012): Degradation and recyclability of poly (ethylene

745   terephthalate). In : Polyester: InTech India, pp. 75–98.

746   Wahab, D. A.; Hussain, A.; Scavino, E.; Mustafa, M. M.; Basri, H. (2006): Development

747   of a prototype automated sorting system for plastic recycling. In *American Journal of*

748   *Applied Sciences* 3 (7), pp. 1924–1928.

749   Yu, Jie; Sun, Lushi; Ma, Chuan; Qiao, Yu; Yao, Hong (2016): Thermal degradation of

750   PVC. A review. In *Waste management* 48, pp. 300–314.

Online Supplementary Files_revised